**Abstract:** We have performed high resolution spectroscopy of rubidium with a single mode continuous wave distributed feedback (DFB) laser diode. The saturation spectrum of the D_2-line of ^{85}Rb and ^{87}Rb was recorded with a resolution close to the natural line width. The emission frequency was actively stabilized to Doppler-free transitions with a relative accuracy of better than 7 parts in 10^9 using commercially available servo devices only. An output power of 80 mW was sufficient to allow for two-photon spectroscopy of the 5S-5D-transition of ^{87}Rb. Further, we report on the spectral properties of the DFB diode, its tuning range and its frequency modulation properties. The line width of the diode laser, determined with high resolution Doppler free two photon spectroscopy, was 4 MHz without applying any active stabilization techniques. For time scales below 5 μs the line width drops below 2 MHz.
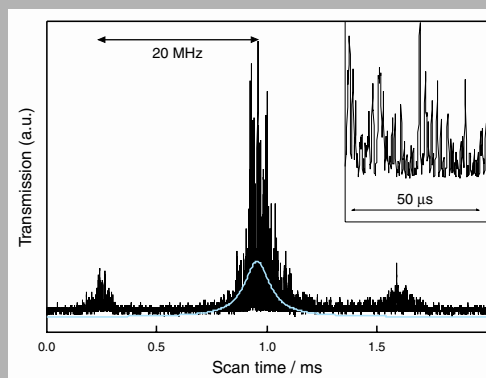
Transmission spectrum of the Fabry-Perot cavity

Rubidium spectroscopy at 778–780 nm with a distributed feedback laser diode

S. Kraft, [1,*] *A. Deninger,* [2] *C. Trück,* [1] *J. Fortágh,* [1] *F. Lison,* [2] *and C. Zimmermann* [1]

[1] Physikalisches Institut, Universität Tübingen, Auf der Morgenstelle 14, 72076 Tübingen, Germany
[2] TOPTICA Photonics AG, Fraunhoferstraße 14, 82152 Martinsried, Germany

The commercial introduction of single mode quantum well laser diodes about 15 years ago has revolutionized high resolution spectroscopy of atoms and molecules. While the spectral properties and the tunability of the pure diode chip are not sufficient for many applications, a reliable and useful device can be constructed by stabilizing the diode with optical feedback from an external grating [1–3]. Today, so-called external cavity diode lasers (ECDLs) are commercially available and widely used in numerous experiments in the fields of quantum optics, ultra-cold atomic and molecular quantum gases, high resolution spectroscopy, and metrology. Although highly superior to conventional laser systems in many aspects, diode lasers still require considerable expertise for alignment, frequency control and operation such that the optical apparatus is still a critical part in a typical experiment. In particular, for mode-hop free tuning over a large frequency range, the Bragg angle of the grating and the resonator length need to be adjusted simultaneously to keep a longitudinal mode resonant within the laser cavity. Although mode-hop free tuning ranges in the order of 100 GHz have been demonstrated with commercially available ECDLs, the precise mechanical realization of the pivot axis remains a challenge in terms of engineering, adjustment and stability.

A semiconductor laser that offers the tunability of an external-cavity system without its mechanical complexity is a Distributed Feed-Back (DFB) diode [4]. In a DFB diode, a Bragg grating is integrated into the active section of the semiconductor. Wavelength tuning is realized by altering the refractive index of the semiconductor, which can be achieved by either changing the temperature or the operating current. This type of laser has long been used for telecommunication and can be regarded as the opti-

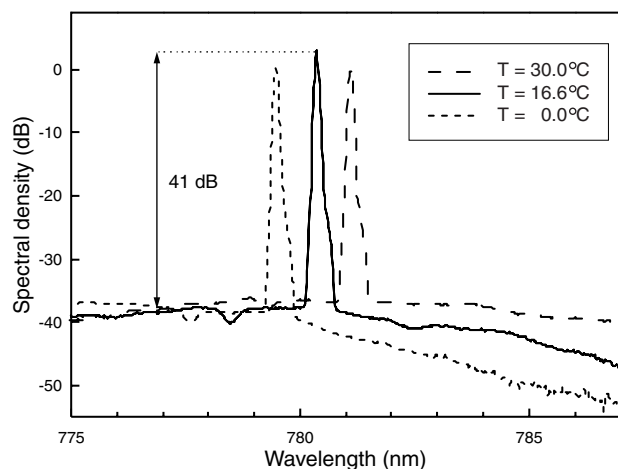* Corresponding author: e-mail: kraft@pit.physik.uni-tuebingen.de

Figure 1 Emission spectra of the DFB laser at different diode temperatures of 0.0°C, 16.6°C, and 30°C (from left to right). The resolution of the grating spectrometer was 0.05 nm
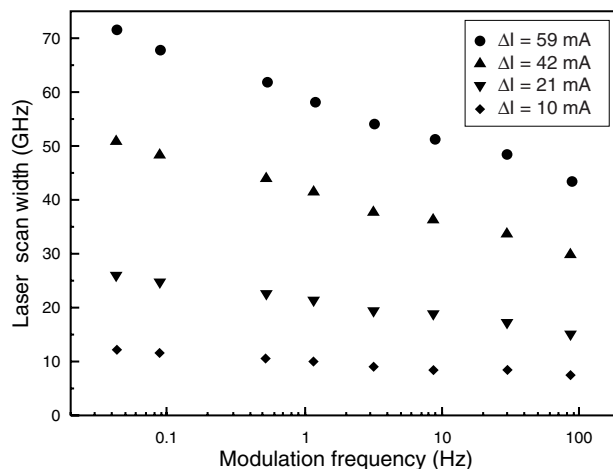

Figure 2 Tuning range of the DFB diode with current modulation. The graph shows the measured scan width as a function of the tuning speed (modulation frequency in Hz). The symbols represent current modulation amplitudes of $\Delta I = 10$ mA, $\Delta I = 21$ mA, $\Delta I = 42$ mA, and $\Delta I = 59$ mA, respectively

cal analogue of a voltage controlled oscillator in radio frequency technology: the emitted wavelength depends only on well controlled parameters in a robust and reproducible way. Whilst DFB diodes at 1550 nm proved suitable for spectroscopy of hydrocarbons [5], spectroscopic measurements with alkali atoms have hitherto required second harmonic generation [6]. Recently, DFB laser chips have become available at various wavelengths near the D_1- and D_2-lines of alkaline atoms. In this article we present a detailed test of a DFB laser for spectroscopy of the rubidium D_2-line and the two-photon 5S-5D transition. It turns out that with low noise driving electronics its performance equals that of grating stabilized diode lasers in almost all aspects. By reducing the complexity of optical experiments, this diode laser opens new possibilities for upcoming projects that require automated operation, e.g. optical clocks in satellites or air-borne experiments in atmospheric physics.

For the measurements presented here, a DL 100 laser system and control electronics from TOPTICA Photonics were used. Experiments were carried out with two different DFB diodes with emission ranges of 779.1–781.0 nm and 777.8–780.3 nm, respectively. The diodes were mounted into a "ColdPack" housing [7], a TO-3 style package with integrated thermistor and four thermoelectric coolers. The ColdPack permitted rapid and flexible control of the diode temperature within a range of $-10\ldots+40^{\circ}$C and sweep times of up to 3.5 K/s. A "Bias-Tee" was included in the laser head to allow for radio frequency modulation of the laser current and the generation of sidebands within the laser spectrum. For frequency stabilization, a lock-in regulator was employed. The laser beam was collimated by an aspheric lens (NA = 0.55). The laser beam profile was shaped from elliptical to circular by an anamorphic prism pair that compressed the long axis by a factor of

three. A 60 dB optical isolator prevented optical feedback into the laser diode.

The coarse spectral properties of the DFB laser were characterized with a commercial grating spectrometer (AQ-6315A Optical Spectrum Analyzer, Ando Electric) and a high precision wavelength meter (HighFinesse-Angstrom WS/Ultimate, absolute accuracy 30 MHz).

Fig. 1 shows the spectrum of the DFB diode at different temperatures as measured with the grating spectrometer at 50 pm resolution. It reveals a background of amplified spontaneous emission (ASE) which is suppressed by $37\ldots41$ dB relative to the coherent part of the diode radiation. At low temperatures, a slight increase in ASE is observed on the short-wavelength side of the spectrum. This results from the difference in the temperature induced frequency shift of the internal grating, which determines the lasing wavelength, and of the gain profile of the semiconductor which is responsible for the ASE. More specifically, the resonance wavelength of the grating changes by approximately 0.05 nm/K (see below), while the gain spectrum varies at a rate of ~ 0.2 nm/K. Thus, the resonant wavelength shifts to the side of the gain spectrum, which eventually limits the accessible wavelength range of the DFB diode.

The tuning range of the laser was determined with the wavelength meter. The output frequency can either be changed by varying the operating current of the diode or the temperature of the chip housing. The modulation of the current changes both the carrier density and the internal temperature of the semiconductor chip. The thermal effect is comparably slow and becomes less relevant with increasing tuning rates. This is shown in Fig. 2, which plots the scan width (i.e. the shift of the emission frequency)
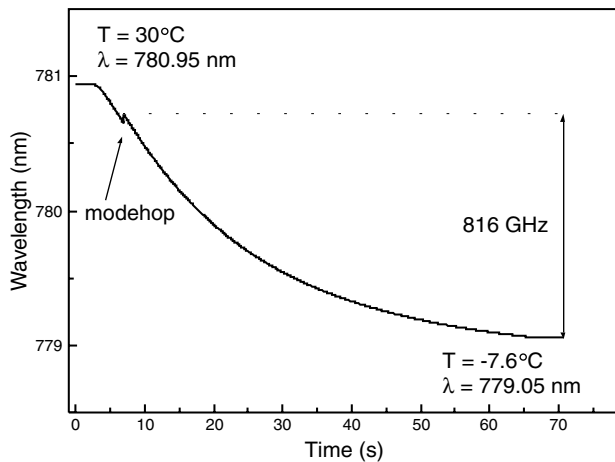
Figure 3 Thermal tuning characteristics of the DFB diode. Shown is the change of the emission wavelength while the diode was cooled from $30°$C to $-7.6°$C. The mean thermal tuning rate is $\Delta\nu/\Delta$T = - 25 GHz/K

Figure 4 Experimental setup of the experiment. The beam of the DFB laser is collimated and passes a 60 dB optical isolator. (a) line width measurements were done using a Fabry-Perot cavity. (b) Setup used for rubidium saturation spectroscopy. For 2-photon spectroscopy (c), the laser is focused into the cell and a photo multiplier is added for detection of the blue fluorescence light

as a function of tuning speed. The different symbols refer to modulation amplitudes of 59 mA, 42 mA, 21 mA, and 10 mA, respectively. All measurements indicate an approximately logarithmic reduction of the scan width with increasing modulation frequency. More specifically, the tuning rate [GHz/mA] amounts to $\approx$ 1.2 GHz/mA at slow modulation frequencies ($f = 42$ mHz) and decreases to $\approx$ 0.7 GHz/mA at faster modulation frequencies ($f = 86$ Hz). Moreover, the tuning rate is independent of the modulation amplitude, i.e. at any fixed modulation frequency, the ratio of the scan widths in Fig. 2 reproduces precisely the ratio of the different modulation amplitudes employed. Generally, the comparatively large tuning rates call for a low-noise current driver for high resolution applications with laser line widths in the 1 MHz range.

The thermal tuning characteristics are illustrated in Fig. 3. The diode temperature was decreased from $30°$C to $-7.6°$C while the emission wavelength was monitored with the wavelength meter. The wavelength varied between 780.95 nm and 779.05 nm, with one mode-hop by 0.06 nm (30 GHz) occurring at 780.7 nm. Single-mode emission was maintained over a wavelength range of more than 1.6 nm (814 GHz). The data yield an average thermal tuning rate of $\Delta\nu/\Delta$T = - 25 GHz/K (+ 0.05 nm/K).

For line width measurements, we used the setup sketched in Fig. 4a. The laser beam was coupled into a Fabry-Perot cavity consisting of two mirrors spaced apart at a distance of 90 cm. The input coupler (nominal reflectivity 99.6%) had a radius of curvature of -2000 mm while the second mirror (nominal reflectivity 99.8%) was plane. Mode matching was accomplished by a lens (f = 1000 mm) placed 10 cm in front of the input coupler. The transmitted light was detected by a fast photo diode with a band width of 40 MHz. For saturation spectroscopy of the rubidium
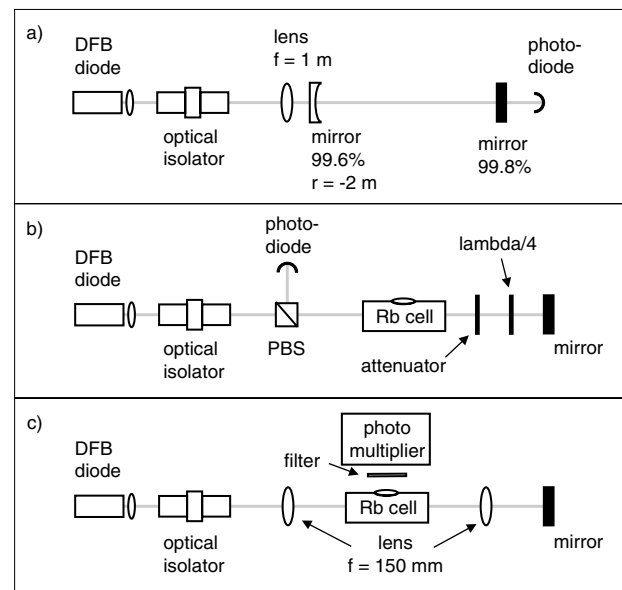
D_2 line, the setup was modified as shown in Fig. 4b. The laser beam successively passed a polarizing beam splitter (PBS), a glass cell filled with rubidium vapor, an attenuator (attenuation factor = 6), and a quarter wave retardation plate before being retro reflected. The probe beam, having passed the retardation plate twice, was coupled out at the PBS and detected by a fast photo diode.

For measurements of the 5S-5D two-photon transition (Fig. 4c), the attenuator and the retardation plate were removed and the beam was focussed and re-collimated by two lenses (f = 150 mm, distance 300 mm). The rubidium cell, placed at the focus, was heated to $\sim$ 100$°$C in order to increase the vapor pressure and the 420 nm fluorescence light from the radiative cascade 5D-6P-5S [8,9] was detected with a photo multiplier.

For the line width measurement of the DFB laser, the laser beam was coupled into the aforementioned Fabry-Perot cavity (free spectral range 166 MHz, estimated finesse > 500). The transmitted light was focussed onto the fast photo diode. In order to provide a frequency reference, side bands were generated by applying a 20 MHz sinusoidal modulation to the laser current by means of a Bias-Tee. In addition the operating current was linearly modulated in order to scan the laser across the resonance of the Fabry-Perot cavity. Fig. 5 shows the transmitted signal versus time. The velocity of the scan can be determined from the position of the sidebands. In the given example
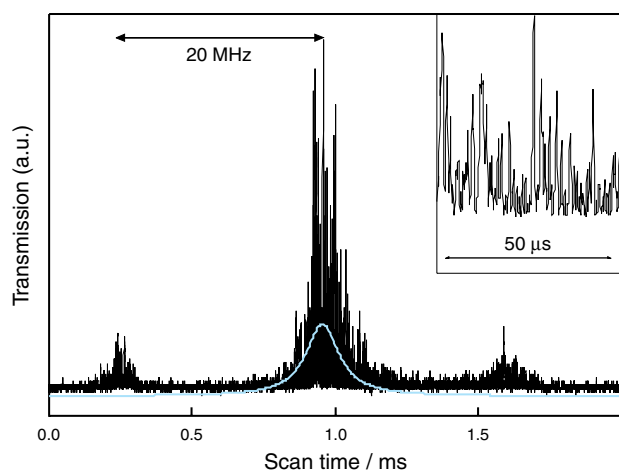
Figure 5 Transmission spectrum of the Fabry-Perot cavity. The laser wavelength was scanned at 30 MHz/ms. The spectrum consists of the main resonance and two sidebands produced by 20 MHz rf-modulation. The inset shows an enlarged view of the main resonance

Figure 6 Saturation spectrum of the D_2-line of ^{87}Rb and ^{85}Rb. The figure shows the four Doppler broadened resonance lines of the transitions ^{87}Rb $F_g = 1$, ^{85}Rb $F_g = 2$, ^{85}Rb $F_g = 3$, and ^{87}Rb $F_g = 2$ (from left to right). The dotted line indicates the intensity modulation resulting from a modulation of the diode's driver current. The inset shows a close-up of the $F_g = 2$ transition of ^{87}Rb. All six Doppler-free peaks are resolved (from left to right: $F_g = 2 \rightarrow F_e = 3$, cross-over $F_e = 2\&3$, cross-over $F_e = 3\&1$, $F_e = 2$, cross-over $F_e = 2\&1$, and $F_e = 1$)

it amounts to 30 MHz/ms. The 70 μs time interval for scanning across the resonance corresponds to a laser line FWHM of 2 MHz. However, the cavity transmission does not form a smooth resonance but rather consists of several sharp needles with an individual width of typically 0.5 μs each. These needles were also observed when the laser frequency was scanned without additional rf modulation. We have investigated the width of these needles for different scanning rates between 30 MHz/ms and 2 GHz/ms. We observed that independent of the scan speed, the width of the resonance envelope remained constant in the frequency domain (2 MHz, line in Fig. 5) while the width of the needles remained unchanged in the time domain (0.5 μs). We then varied the laser current and found a strong influence on the line width. Starting with a rather broad (8 MHz) line at 45 mA (output power P = 10 mW) the line width decreased with increasing current and reached a minimum for values between 60 and 80 mA (P = 35 mW). At higher currents the line width increased again. We thus conclude that the observed line width of the envelope is a technical line width, which results from frequency "jumps" of a narrow laser line. The jumps may be due to spatial hole burning, which leads to inhomogeneities in the charge carrier density and consequently to mode fluctuations [10, 11]. The observed constant needle width in the time domain is consistent with a model for the laser spectrum that consists of a very narrow frequency component which randomly sweeps across the cavity resonance in a time interval shorter than the cavity filling time. The observed width of 0.5 μs corresponds to a cavity line width of 300 kHz which agrees reasonably well with the expected line width of 200 kHz. This value also defines an upper limit for the laser spectrum at time intervals shorter than 0.5 μs. For in-
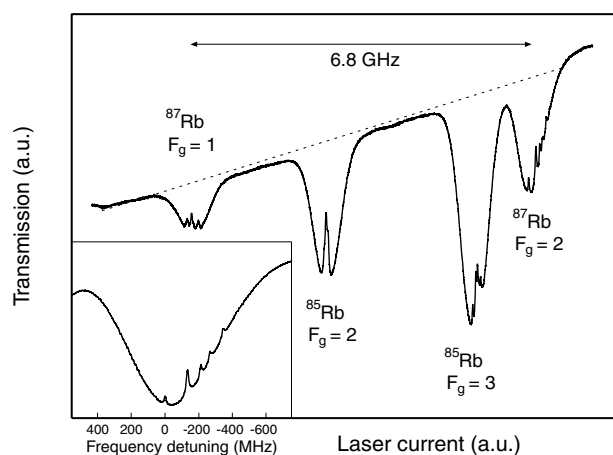
tervals of up to 5 μs the frequency excursion of the jumping component remains within 2 MHz as can be seen from the envelope. From spectroscopic data (see below) one can infer that the excursions always stay within a range of 4 MHz.

In order to test the laser in a spectroscopic application, we recorded the saturation spectra of the rubidium D_2 line (Fig. 6). The intensities of pump and probe beam were 5 mW and 150 μW respectively, the beam diameters were approximately 1mm. The spectra were acquired by scanning the current of the diode. The current variation of 6 mA resulted in a corresponding intensity change of 10% within the scan range of 8.4 GHz. The laser power varied nearly proportional with the current as shown in the figure. The four Doppler broadened lines correspond to excitation of the two rubidium isotopes ^{85}Rb and ^{87}Rb with two hyperfine ground states each: ^{87}Rb ($F_g = 1$), ^{85}Rb ($F_g = 2$), ^{85}Rb ($F_g = 3$), and ^{87}Rb ($F_g = 2$). Their half widths of 700 MHz reflect the gas temperature of 300K. Each resonance features several Doppler-free peaks, as shown in the inset of Fig. 6 for the ^{87}Rb $F_g = 2$ transition. The measured line width of the hyperfine transitions and crossover-resonances is 9 MHz, which is close to the natural line width of 6 MHz.

A lock-in servo loop was used to stabilize the laser frequency to Doppler-free D_2-line transitions from the ^{87}Rb ($F_g = 2$) ground state. The DFB laser was successively locked to the transition $F_g = 2 \rightarrow F_e = 3$ and the two cross-over resonances $F_g = 2 \rightarrow F_e = 2\&3$ and $F_g = 2 \rightarrow F_e = 1\&3$ while the wavelength was recorded

Transition	Av. time [min:s]	Literature value [THz]	Measured mean [THz]	Difference [MHz]	Freq STD [MHz]	Relative stability
F= 2 →F' = 3	4:38	384.228 115 2	384.228 127 8	12.6	1.3	3.5×10^{-9}
F= 2 →F' = 2 & 3	30:27	384.227 981 9	384.227 992 9	11.0	2.4	6.4×10^{-9}
F= 2 →F' = 1 & 3	5:21	384.227 903 4	384.227 912 4	8.0	1.6	4.3×10^{-9}

Table 1 Frequency-locking of a DFB laser to Doppler-free resonance lines of ^{87}Rb, transition $5S_{1/2} \rightarrow 5P_{3/2}$. Literature values are taken from [12]. The time interval over which the laser frequency has been averaged is shown in the column labelled "Av. time". "Measured mean" denotes the average value measured by the wavelength meter while the laser was locked to the respective transition. The differences between the literature reference and our measurement are shown in the fifth column. "Freq STD" gives the measured standard deviation of the laser frequency while the laser was in lock. The last column states the relative frequency stability for the different lock periods
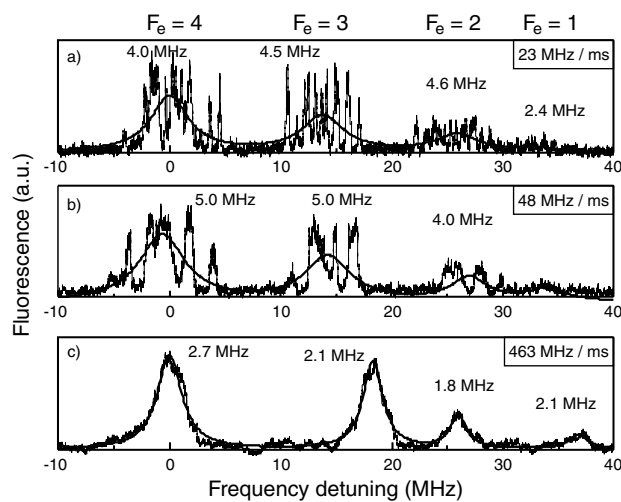

Figure 7 Hyperfine spectrum of the two-photon transition $5S_{1/2}$ ($F_g = 2$) to $5D_{5/2}$ ($F_e = 4$ to 1) of ^{87}Rb. The graph shows spectra acquired with different scan speeds of 23 MHz/ms, 48 MHz/ms, and 463 MHz/ms, respectively. At slow scan frequencies, the resonance lines broaden and are successively decomposed into multiple peaks resulting from high-frequent wavelength hops of the DFB diode. Also shown are best-fit curves of the data. The line width determined from a Lorentzian fit is given for each resonance

with the wavelength meter. Table 1 compares precision data taken from literature [12] with our recorded values. The deviation of the measured frequencies from the literature values of approximately 10 MHz is well below the accuracy of the wavelength meter which was calibrated with a stabilized helium-neon laser at 632.99 nm. With the laser being locked to the respective resonances, values between 1.4 and 2.5 MHz were measured for the standard deviation of the frequency. This translates into a relative frequency stability of 3–6 parts in 10^9. However, as the resolution of the utilized wavelength lies within the same range, the actual frequency stability can be assumed to be even better.

The 5S-5D two-photon transition of rubidium offers a narrow line width (∼500 kHz) [9] due to the long life-

time of the 5D state. To probe this transition we focussed the laser beam into the spectroscopy cell and modulated the wavelength by scanning the operating current. Fig. 7 shows the fluorescence signal, measured with a photo multiplier, after excitation of the $5S_{1/2}$, $F_g = 2 \rightarrow 5D_{5/2}$ transition of ^{87}Rb. Spectra a) – c) were recorded with scan speeds of 23 MHz/ms, 48 MHz/ms, and 463 MHz/ms, respectively. Also shown is a fit curve of the four Lorentzian line profiles. The x-axis of the plot is scaled to the frequency detuning using the frequency separation between the $F_e = 4$ and $F_e = 2$ peaks.

At slow scan speeds (a), the resonance lines are decomposed into multiple peaks due to jitter of the laser frequency. As observed in the Fabry-Perot spectrum (Fig. 5), the width of each needle within the time domain does not depend on the scanning speed. By scanning faster (b), the width of the line envelope remains unchanged, while the number of needles per resonance decreases. At even faster scan speeds (c), each resonance consists of only one needle. The frequency hops now result in a displacement of the line in frequency space. The fit curves of the peak structure in Fig. 7 can be employed to investigate the technical line width of the DFB diode as a function of scan velocity. The minimum FWHM width of the measured lines is approximately 1.5–2 MHz. This value is broader than the natural line width of 500 kHz, and agrees with the previous measurements with the Fabry-Perot cavity (Fig. 5). At even higher scan speeds, the width of the spectral signatures appears to be Fourier limited, leading to line rebroadening.

In summary, it can be stated that the type of laser described here is very suitable for almost all standard high resolution applications in alkali spectroscopy including laser cooling and optical manipulation of ultra cold atoms. The high output power allows for efficiently driving nonlinear processes and the spectral width of the bare chip lies well within the natural line width of the D_1 and D_2-transitions. The relatively low frequency noise of the laser spectrum probably allows for further reducing the spectral width to well below 100 kHz with standard servo loops that link the injection current to an error signal derived from an atomic spectrum or a stable resonator. The absence of any critical mechanical or optical components in

the laser's control system permits a very reliable and stable operation. Together with its extremely large mode-hop free tuning range these properties will probably allow for the construction of compact and sophisticated optical radiation sources that transfer the reliability and performance known from radiofrequency technology into the optical domain.

References

[1] C.E. Wieman and L. Hollberg, Rev. Sci. Instrum. **62**, 1 (1991).

[2] K.B. MacAdam, A. Steinbach, and C. Wieman, Am. J. Phys. **60**, 1098 (1992).

[3] L. Ricci, M. Weidemüller, T. Esslinger, et al., Opt. Commun. **117**, 541 (1995).

[4] Y. Tohmori, F. Kano, H. Ishii, et al., Elect. Lett. **29**, 1350 (1993).

[5] M. de Labachelerie, K. Nakagawa, and M. Ohtsu, Opt. Lett. **19**, 840 (1994).

[6] M. Poulin, C. Latrasse, M. Têtu, and M. Breton, Opt. Lett. **19**, 1183 (1994).

[7] G. Bickleder, A. Zach, and W. Kaenders, Patent DE 199 26 801 (2000).

[8] R.E. Ryan, L.A. Westling, and H.J. Metcalf, J. Opt. Soc. Am. B **10**, 1643 (1993).

[9] F. Nez, F. Biraben, R. Felder, and Y. Millerioux, Opt. Commun. **102**, 432 (1993).

[10] X. Pan, H. Olesen, and B. Tromborg, IEEE Photon. Tech. Lett. **2**, 312 (1990).

[11] H. Wenzel, H.J. Wünsche, and U. Bandelow, Electron. Lett. **27**, 2301 (1991).

[12] D.A. Steck, http://steck.us/alkalidata, Revision 1.6 (2003).